

GROUND MOTION MODEL FOR THE LHC

A. Verdier and L. Vos, CERN, Geneva, Switzerland

Abstract

A ground motion model based on geo-physical arguments is presented. The purpose of this model is to predict possible beam separation in the interaction regions of the LHC due to ground motion developing in time spans in the order of seconds to hours. Although this model can also be used to predict statistical movement of accelerator objects on a larger time scale (yearly alignment) its usefulness for that part of the spectrum is questionable. This is simply due to the fact that other perturbations largely dominate basic ground motion effects.

1 INTRODUCTION

The frequency range of ground motion that is of interest for the LHC is extremely large. On the high frequency side it involves frequencies in the kHz region where the quadrupole motion couples with the lowest harmonics of the betatron tune and may lead to emittance growth. This effect is documented and has been taken into account for the design of the transverse feedback system [1]. Next there is the narrow band plane wave excitation where the ground motion wavelength matches the betatron wavelength [4] and involves frequencies in the order of $1 Hz$. This effect is negligible for the LHC[1]. Then we must consider the uncorrelated motions or vibrations in the range between $1 Hz$ and $30 \mu Hz$. They are responsible for orbit deformations which in the case of the 2 channel LHC may lead to beam separation and loss of luminosity.

The performance of the LHC depends critically on the orbit behaviour in the $1 Hz$ to $30 \mu Hz$ region. The *ATL* law [5] is not applicable for the full range. In order to improve our predictive power a true physical model of ground motion[2] has been developed that covers the specified frequency span.

Then there is the frequency range in the order of $30 nHz$ which is of interest for many machines since it involves the need of periodic repositioning of machine elements. Observations seem to show that the influence of local traumatism and environmental effects dominate basic ground motion in this frequency regime. It is questionable whether the model can be applied in practice in this range as well.

2 GROUND MOTION MODEL

A typical ground motion power spectrum is sketched in Fig 1. The *ocean well* spectrum that stands out and extends from less than 0.1 to $1 Hz$ is known to be

coherent. That is not surprising. Indeed, the high-pass cut-off frequency of $\sim 0.2 Hz$ together with the acoustic speed in water ($1.5 km s^{-1}$) suggest a limiting wavelength in the oceans of around $\sim 7 km$, not very different from the depth of the abyssal plain (between 3 and $5.5 km$ [6]). Clearly, these waves are surface waves and it is very difficult to imagine geological fault structures that would cause these waves to loose coherence over a fraction of a wavelength. Thus it is safe to remove the powerful ocean well spectral peak from the model since only the uncorrelated movements are a concern for the problem at hand.

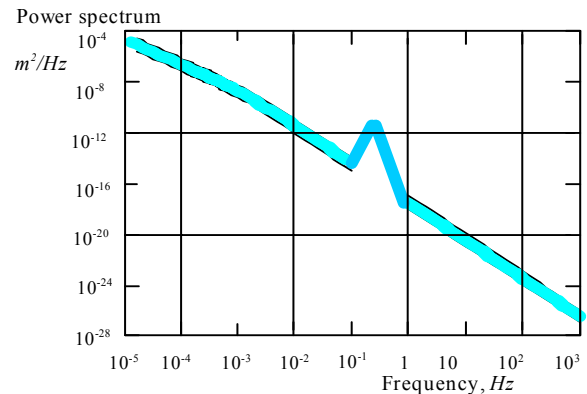


Figure 1 : Typical ground-motion power spectrum.

The remaining spectrum tends to fall with frequency as f^{-3} at frequencies above the *ocean hum*, while the frequency slope reduces to f^{-2} well below this [9]. Notice that the wavelengths involved in the latter case exceed $25 km$. However, clear evidence exists on lack of correlation (randomness) of very low frequency noises at distances much less than the wavelength. The model has to fit two specifications. The first one is concerns the general formulation of the motion of a single point. The second one is related to the randomization of the low frequency earth movements.

2.1 Basic model

The model consists of two building blocks, an excitation source and a transfer function. They will be discussed below.

2.1.1 Transfer function

The maximum seismic length of the earth is $\sim 1500 s$ [3]. The seismic 'depth' of the earth is about $1/3$ of this [6] and hence defines a *cut-off* frequency of $f_{co} \sim 1/500 = 2 mHz$. This is confirmed by the far away *amplitude* response of earthquakes. Fig.2 is taken from [10] and is a typical example. The response is compatible with a high-

pass filter behaviour with an amplitude cut-off $\omega_{co} \sim 1/400$ rad/s, hence a cut-off frequency of $f_{co} \sim 0.8$ mHz for power of displacement (amplitude²). This suggests an average high pass cut-off $f_{co} \sim 1.5$ mHz. It is worthwhile to note at this point that the seismic wave attenuation with distance is very small.

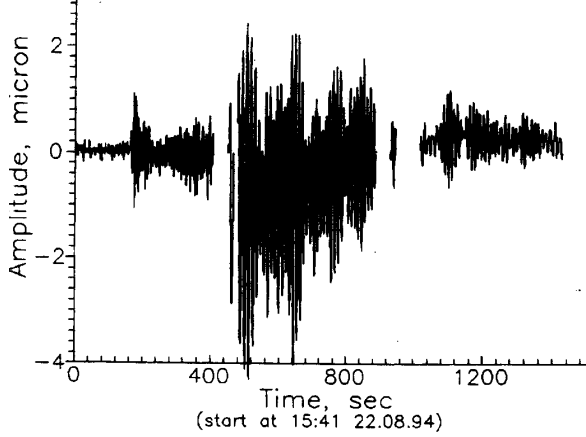


Figure 2 : Typical faraway response to earthquake. The fast oscillation is the response of the oceans pounding on the continents.

2.1.2 Excitation source

Microseismic noise and earthquakes are blended into a single family and constitute the excitation source of the problem at hand. The examination of a substantial body of phenomenological material concerning earthquakes has lead to the Gutenberg- Richter law[3,6]:

$$\log(n) = -M, \quad (1)$$

where n is the number of earth quakes in a given time and a given area with a magnitude M or larger. It is easy to see that this law formulated in that way corresponds with a f^{-3} power density spectrum. Indeed, $n \sim 1/f$ and $x^2 \sim M^2$, hence differentiating with respect to f yields the f^3 dependence. The response of the earth to the seismic excitation in terms of a power density can then be expressed by the following function which combines the high-pass filter transfer function and the source spectrum:

$$\frac{dx^2}{df}(f) = \frac{k_{gm}}{f^2 \sqrt{f_{co}^2 + f^2}} [m^2/Hz], \quad (2)$$

The factor k_{gm} is a non-local quantity that varies with time from $\sim 10^{18} m^2/s^2$ to $\sim 10^{16} m^2/s^2$ depending on the state of global excitation. This power spectrum is shown in Fig.3 together with a number of observations taken from [7].

2.2 Randomness

The question now arises how two points, close together (much less than a wavelength), can move independently? From earthquake observations it is known

that the depth of the sources is very often ~ 30 km (the Moho discontinuity[6,8]). This and the geographical spreading of the sources may explain the fact that the response can be incoherent while, as was pointed out before, shallow surface waves (ocean pounding on continental shelf) are always coherent. In fact it is known that the randomness of the differential movement at a given location depends strongly on the fractured state of the site. The surface behaves as a number of independent blocks that are excited from below. That is borne out clearly by the experimental observation on two points on either side of a construction joint[11].

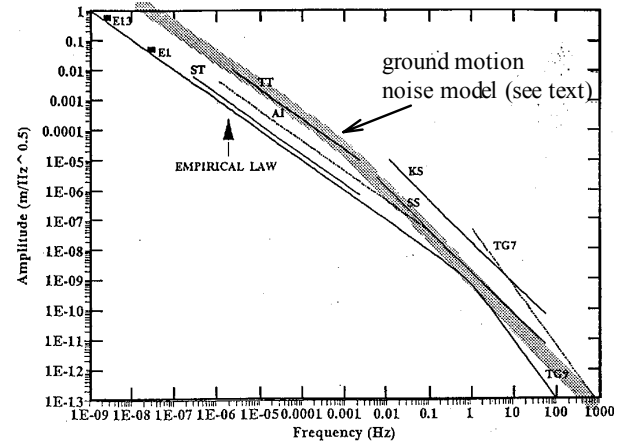


Figure 3 : Comparison with basic ground-motion model and observations. The line marked 'empirical law' is related to the model proposed in [7].

This then leads naturally to the notion of coherence length L_{ch} . That length has to be understood in a statistical sense: two points at a distance smaller than L_{ch} are likely to move coherently, while two points which are further away are likely to move incoherently. The notion of coherent length is well suited for accelerators where local differences will average out.

The coherence length can be determined from orbit measurements. The only assumption to be made concerns k_{gm} . It was put at $k_{gm} = 10^{18} m^2/s^2$. The integration of Eq. 2 in frequency from infinity to $f=1/t$ yields the power of displacement of a single element:

$$dx^2(t) = \frac{k_{gm}}{f_{co}^2} \left(\sqrt{1 + (f_{co}t)^2} - 1 \right). \quad (3)$$

The orbit deformation can be found simply by multiplying Eq. 3 with the optical amplification factor $O_A = (\beta Kl / 2 \sin(\pi q))^2 N$, where β is the optical function at a quadrupole and Kl its integrated focalisation force. N is the number of uncorrelated blocks around the accelerator which is at the maximum the number of F or D quadrupoles. From [12] (known effect of superconducting insertion quadrupoles removed) it was possible to estimate the local value of L_{ch} in LEP at 130 m.

Eq. 3 allows the computation of the *rms* half separation between the beams as a function of time. This can be expressed in terms of the *rms* beam size σ . In normal, quiet conditions the rate of separation is such that 0.5σ is reached after nearly 8 hours (Fig 4). It is to be expected that once in a while the global system is highly excited ($k_{gm} = 10^{-16} \text{ m}^2/\text{s}^2$). In that case the rate of separation is about a factor of 10 larger (Fig 5) and the same separation is reached in 500 s where the effect is linear in time. Clearly procedures must be ready in order to cope with such a rate of separation.

half sep. / σ

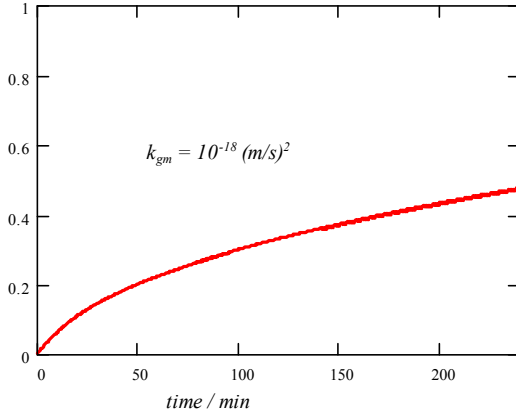


Figure 4 : Expected half separation of the beams in the LHC for *normal* level of excitation of ground motion.

half sep. / σ

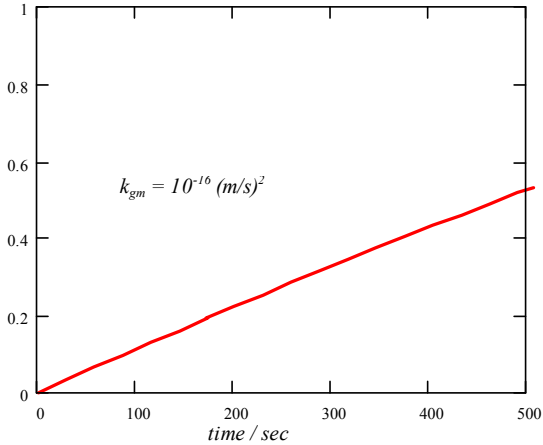


Figure 5 : Expected half separation of the beams in the LHC for *high* level of excitation of ground motion.

3 GROUND MOTION MODEL IN THE *nHz* REGION?

It is worth to note that the ground motion model presented above is to a large extent compatible with the *ATL* law for frequencies below 1 *mHz* [10]. Indeed, observing that $f \sim 1/T$ and noticing that for propagating ground waves $L \sim T$, hence $L \sim 1/f$, the *ATL* law is equivalent to a $1/f^2$ dependence [10]. Contrary to what is argued in

[13] it is shown below that the processing of the alignment data and the effect of random measurement errors mimic the *ATL* conjecture.

3.1 Processing the data

The raw alignment data are first referred to the best plane, i.e. that which minimises the distances to it. This is innocuous. Then they are corrected in order to obtain the same position of the first magnet after one turn (correction of the closure error). Another processing has been applied to these data in [13]: the lowest five Fourier harmonics are subtracted. This is probably equivalent to measuring the misalignments with respect to a smooth curve. The two last processings are not innocuous.

The effect of a subtraction can be estimated as follows. By definition [13], the r.m.s. over the circumference of length C of the height difference at two positions separated by the length L is :

$$dH_R^2(L) = \int_0^C [y(s+L) - y(s)]^2 ds$$

If some function $f(s)$ is subtracted from the positions $y(s)$, we obtain :

$$dH_K^2(L) = \int_0^C [y(s+L) - f(s+L) - y(s) + f(s)]^2 ds$$

Expanding the square and noting that :

- the functions $f(s)$ and $y(s)$ are uncorrelated
- the integral of $y(s)$ is zero

we obtain eventually :

$$dH_K^2(L) = dH_R^2(L) + \int_0^C [f(s+L) - f(s)]^2 ds \quad (4)$$

For the case of the correction of a closure error of value cl , the function $f(s)$ is given by $f(s) = cl \times s/C$. From Eq. 4 the error on $dH_K^2(L)$ is given by $cl \frac{L^2}{C^2}$. It is worth noting that it is quadratic in L , so such an error would produce a curvature in the "variance curve" [13] which is not observed.

For the case of the subtraction of an harmonic of order n and amplitude a , $f(s)$ is given by $a \times \sin(2\pi ns/C)$ and the correction to $dH_K^2(L)$ is given by $2a^2 \sin^2(\pi nL/C)$. For $n=5$ it is easy to see that the curve representing this function has a quasi-linear behaviour in a large part of the range of $\{0, 1\text{km}\}$. Depending on the value of a , in the range of millimeters, this subtraction, which is different for different measurements, can make a difference as large as that attributed to a random variation with time in [13].

3.2 Random walk effect

The random errors in the measurements of the position of a given magnet with respect to the previous one add up like a random walk, i.e. proportional to the square root of the number of measurements. This of course was not ignored in [13].

The random measurement error can be estimated by inspecting the closure errors measured at different periods. From 1993 to 1998 they are 4.0, 0.8, 3.0, 0.8, 0.8, 2.8mm. The average is 2mm with an r.m.s. deviation of 2.2mm. The random walk coefficient associated with the average is $2^2/26.66\text{mm}^2/\text{km}$, i.e. the number in [13]. This makes an A coefficient for 6 months of $0.9 \times 10^{-5} \mu\text{m}^2 \text{s}^{-1} \text{km}^{-1}$ i.e. the value obtained [13].

Furthermore, it has been shown that the random walk effect can produce an apparent spatial low frequency displacement in the millimeter range (see Fig. 9 in [14]).

3.3 *Are the basic very low frequency ground motion power spectra completely absent from alignment data?*

In [14] a massive amount of alignment data for LEP are presented and analysed and they are found to be in agreement with the previous paragraphs for most of the data. From the basic low frequency basic ground motion rms differential displacements of $dx^2 = 0.04 t_{\text{year}} \text{mm}^2$ are expected, where t_{year} is the time counted in years, the typical time scale of machine alignment. It is clear that most of the measured displacements are quite a bit larger than this [14]. Nevertheless, it is interesting to note that signs of basic ground motion activity of the right order of magnitude may be spotted in *quiet* areas of LEP, typically between IP4 and IP5 as apparent in some of the figures in [14].

3.4 *To be kept in mind for LHC*

The history of the LEP tunnel, in which LHC will be installed, is well known. A decisive step forward was accomplished in 1993 when the consequences of proposed LEP realignments were directly analysed. The procedure consisted of converting the survey data into MAD [15] commands and computing the consequences they had on the LEP optics. **For LHC it is essential that this procedure be automated from the beginning of the LHC life.**

A code to analyse the closed orbit distortions has been developed for LEP [16]. It made it possible to detect the large ground motion between IP7 and IP8 in spite of the bad alignment of the machine in 1992. **For LHC it is essential that this program be implemented in the LHC control system from the beginning of the LHC life.** This will make it possible to detect quadrupole misalignments with confidence and to follow up more easily the deformations of the tunnel.

REFERENCES

- [1] L. Vos, *Effect of Very Low Frequency Ground Motion on the LHC*, EPAC98, Stockholm, 1998
- [2] L. Vos, *Ground Motion in LEP and LHC*, Particle Accelerators, Volume 50, 1995.
- [3] G. E. Fischer, *Ground Motion and its Effect in Accelerator Design*, AIP Conference Proceedings 153, 1984.
- [4] G. E. Fischer and P. Morton, *Ground Motion Tolerances for the SSC*, SLAC-PUB-3870, 1986.
- [5] B.A. Baklakov et al, *Investigation of Seismic Vibrations and Relative Displacements of Linear Collider VLEPP Elements*, Particle Accelerator Conference, San Francisco 1991.
- [6] W.K. Hamblin, *Earth's Dynamic Systems*, 6th ed., Macmillan PC, 1992.
- [7] S. Takeda et al, *Slow Drift and Frequency Spectra on Ground Motion*, KEK Preprint 93-61, 1993.
- [8] *Géologie Générale*, Instituts Romands des Sciences de la Terre.
- [9] S. Takeda et al, *Slow Ground Motion and Alignment System*, KEK Preprint 94-48, 1994.
- [10] V.M. Juravlev et al., *Seismic Conditions in Finland and Stability Requirements for the Future Linear Collider*, Report Series HU-SEFT R 1995-01, 1995.
- [11] S. Takeda and M. Yoshioka, *Ground Motion at KEK*, KEK Preprint 95-209, 1996.
- [12] F. Tecker, *Low-beta quadrupole movements as source of vertical orbit drifts at LEP*, CERN-SL/96-40 (BI), 1996.
- [13] V. Shiltsev, *Space-time ground diffusion : the ATL law for accelerators*. Proc. of the fourth Int. Workshop on accelerator alignment IWAA95, KEK, November 1995. KEK Proceedings 95-12 (January 1996).
- [14] R. Pitthan, *LEP Vertical Tunnel Movements-Lessons for Future Colliders*, CLIC Note 422,
- [15] H. Grote and F.C. Iselin, *The MAD program (Methodical Accelerator Design) version 8.16, User's reference manual*, CERN/SL/90-13(AP), (rev. 4) (March 27, 1995).
- [16] A. Verdier and J-C. Chappelier, *An Automatic Finder of Field Defects in Large AG Machines*, PAC Washington, 1993.